JTTEE5 14:39-44
DOI: 10.1361/10599630522404
1059-9630/$19.00 © ASM International

Fluid Dynamic Effects on Plasma Torch Anode Erosion

X. Sun and J. Heberlein

(Submitted February 11, 2004; in revised form June 25, 2004)

Anode erosion in plasma spray torches results in coating deterioration. The usable life of a torch anode is strongly dependent on the fluid dynamic behavior of the plasma inside the torch, which in turn depends on the geometric design of the anode and the operating parameters. To study the relative importance of these effects, cold flow investigations have been performed with a torch having a glass anode with the same geometric dimensions as a commercial plasma torch. The density differences between the arc and the cold gas were simulated by injecting heated helium from the tip of the cathode into the cold argon gas flow from the regular gas injector. Flow visualization was achieved by seeding the flow with micron-sized particles. A finite-element computational fluid dynamics code was used to simulate the cold flow structure. The results were compared with erosion patterns observed with an actual plasma torch. The results indicate that recirculation eddies inside the torch will force a preferred anode attachment, which is different for different gas injectors. The minimization of such recirculation regions by appropriate fluid dynamic design will result in more random attachment of the arc and prolonged anode life.

Keywords anode erosion, cold flow simulation, computational fluid dynamics, flow visualization, plasma torch

1. Introduction

Anode erosion in plasma spray torches can strongly influence coating quality. Moreover, the effects on the spray process may lead to a reduction in deposition efficiency and increases in coating porosity before the traditional means of controlling the process, such as current, arc voltage, and increases in the torch cooling water temperature, indicate any changes. Numerous ways of reducing the erosion effects through torch design changes have been proposed and implemented. Torches operating with lower arc currents will have less erosion, but usually also lower deposition rates. The swirl flow of the plasma gas has been widely adopted, and it leads to a strong reduction in anode erosion due to a constant movement of the arc (i.e., anode attachment). Using a solenoid magnetic field exerting a Lorentz force on the arc attachment and forcing it to move has a similar effect as the swirl flow plasma gas injection and is widely used, particularly with higher-power torches. A newer development uses three parallel arcs with three anode attachment spots, achieving a similar effect as the distributed heat flux due to vortex flow but with less variation in torch power (Ref 1). All of these developments have been performed based on a qualitative knowledge of the physical processes inside the plasma torch. While there have been numerous efforts to characterize plasma spray jets (e.g., Ref 2), efforts to characterize the plasma inside the torch have been limited due to the difficulty of obtaining optical access through a water-cooled nozzle, and due to the three-dimensional behavior of the arc that makes modeling approaches very complicated. Modeling efforts have concentrated on describing two-dimensional geometries, and turbulent behavior has been described using k-epsilon models (Ref 3-5). Recently, significant progress has been made in the description of flows inside plasma torches using three-dimensional models (Ref 6-8). However, the difficulty associated, in particular, with the cathode region where the cold flow impinges on the hot, low-density arc plasma, and with the unstable anode region has required simplifying assumptions.

This article presents a study in which optical observations of the flow inside the torch are combined with a three-dimensional finite-element model of the fluid dynamics. The observations have been carried out with a torch with a glass anode and using cold flow with a comparable Reynolds number as the plasma flow. The density difference is simulated by using different gases in the center of the flow and in the boundary layer. The results from these investigations have been compared with the erosion behavior in an actual plasma torch operated under comparable conditions. In the following section, the experimental setup and conditions are described. The modeling effort is described next, followed by a presentation and discussion of the experimental results. A summary of and conclusions from this study are presented at the end. Details of the experiment and the results can be found in a recently completed thesis (Ref 9).

2. Description of Equipment

For the cold-flow experiments, a torch has been used that simulates the flow conditions in a Praxair/TAFA SG 100 spray torch (Tafa, Inc., Concord, NH) (i.e., all of the inside dimensions and plasma gas flow passages are identical to those in the commercial torch). The main body has been machined out of a trans-

The original version of this article was published as part of the ASM Proceedings, *Thermal Spray 2003: Advancing the Science and Applying the Technology,* International Thermal Spray Conference (Orlando, FL), May 5-8, 2003, Basil R. Marple and Christian Moreau, Ed., ASM International, 2003.

X. Sun and **J. Heberlein,** University of Minnesota, Minneapolis, MN; Contact e-mail: jvrh@me.umn.edu.

parent plastic, and the anode nozzle (shaped after a Praxair/TAFA 2083-720 anode) has been made of glass. The glass tube has been glued to the plastic main body. The cathode has been machined out of aluminum with a shape identical to that of a Praxair/TAFA1083-129 cathode. However, a channel inside the cathode and an orifice on its tip allowed the injection of gas from the cathode tip into the gas stream. The regular commercial gas injector has been used with three different arrangements: (1) four holes in a straight flow arrangement, (2) four holes in the standard swirl flow arrangement, and (3) eight holes in the swirl flow arrangement.

2.1 Selection of the Operating Parameters

For simulating the plasma flow, two conditions have been found to be important. First, the density gradient between the hot plasma in the arc and the surrounding cold gas in the boundary layer has a strong influence on the fluid dynamic behavior inside the torch and needs to be simulated. For this purpose, a channel model has been adopted with a channel of helium (HE) gas representing the arc plasma, injected into the flow at the tip of the cathode, while the cold gas in the boundary layer is argon (Ar) flow injected through the gas injector at the base of the cathode. In a real torch, the density ratio between the center part of the flow and the boundary layer part has been estimated to be 0.02 to 0.06 (Ref 10). For an Ar temperature of 300 K, an appropriate density ratio of He to Ar of 0.05 is obtained if the He is heated to about 600 K by passing the flow to an electrically heated tube.

For the selection of the mass flow rates, again a two-channel model has been adopted, and the flow rates chosen such that the same Reynolds numbers are obtained for the cold flow as for the flow in the central channel. For the plasma flow, a velocity of 600 to 800 m/s is taken with a mean temperature of 10,000 to 12,000 K, with a diameter half of the 8 mm channel, giving a range of Reynolds numbers of 50 to 100. For the boundary layer, the gas velocity has been assumed to be 200 to 400 m/s, having a mean temperature of 2000 to 5000 K, giving Reynolds numbers of 1000 to 4000. Accordingly, flow rates in the ranges of 4.6 to 8.5 standard liters per minute (sLm) for He, and of 7.55 to 10.97 sLm for Ar were chosen. These flow rates are controlled by MKS mass flow controllers (MKS Instruments, Wilmington, MA).

2.2 Flow Visualization

The flow structures have been made visible by seeding the argon flow with Teflon (DuPont, Wilmington, DE) particles with mean particle diameters of about 3 μm (FLUO HT; Micro Powders Inc., Tarrytown, NY). The particles are introduced into the gas flow with the aid of a Laskin nozzle. In this device, gas is bubbled through a suspension of the particles in water, and small droplets of water are generated containing the particles. A cyclone removes the larger droplets, and the gas flow with the remaining droplets is injected into the Ar flow. The water carrying the droplets evaporates, leaving the Ar with a low percentage of water vapor and with the micron-sized Teflon particles inside the torch.

The flow structures that were made visible by the suspended particles were recorded with a charge-coupled device camera with a zoom lens, and using backlighting of the flow. In most cases, the best information could be obtained by observing the patterns in which the particles deposited on the wall, and photographs of these patterns were taken after a run of 2 to 3 min for subsequent analysis.

2.3 Plasma Torch Experiments

The experiments for comparing the cold-flow results with actual plasma spray torch erosion characteristics have been performed with a Praxair/TAFA SG 100 torch with a 2083-720 anode, a 1083-129 cathode, and the same three flow injectors as used in the cold-flow experiments. Experiments were performed with an arc current of 800 A and an Ar/He mixture with 49/21 sLm. The torch was operated with a new anode for a time between 1 and 10 h. Operating duration was usually ≥1 h, and the effects of arc initiation were minimized. After determination that the anode nozzle showed clear erosion patterns, the anode was sectioned and the erosion patterns were analyzed.

3. Flow Calculations

The three-dimensional flow structures inside the torch have been calculated using the commercial computational fluid dynamics (CFD) code ANSYS-FLOTRAN (ANSYS, Inc., Southpointe, PA). A slightly simplified geometry has been assumed consisting of two cylinders with the nozzle diameter and the diameter of the flow channel surrounding the cathode, respectively. A conical section combined these two cylindrical parts. Laminar flow and a uniform temperature were assumed. A Cartesian coordinate system has been used with x being the direction of the nozzle axis and z being the direction perpendicular to the paper plane. A strongly nonlinear mesh was chosen with high grid-point densities in the injection region and in the region between the cathode tip and the corner between the converging and the straight section of the anode. The fluid properties have been assumed as constant at the injection conditions (i.e., at 300 K for Ar and at 600 K for He). The boundary conditions have been specified such that they describe the experimental conditions.

Figure 1 shows as an example for the results of the velocity

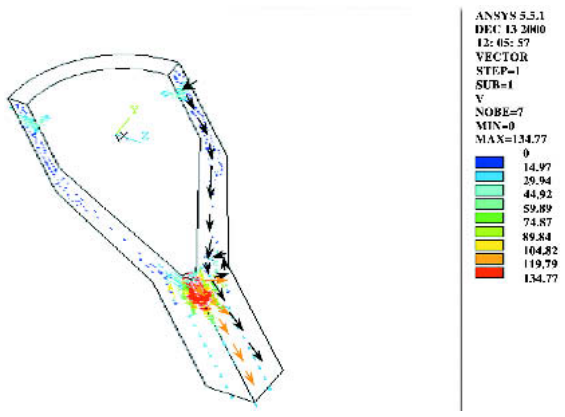

Fig. 1 Velocity vector distribution inside an SG 100 plasma torch with a cold-flow, four-hole straight gas injector, 8.87 slm of Ar flow, and 5 slm of He flow. p = 1 atm at the nozzle exit, and the actual velocities at the injection holes have been used. No slip conditions have been used for the wall boundaries.

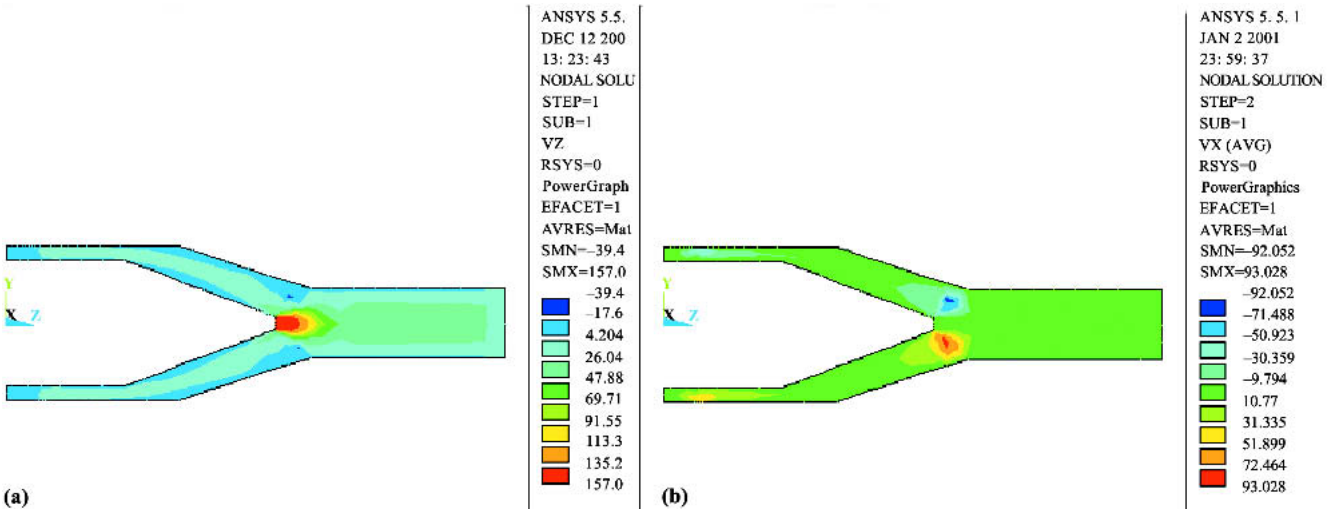

Fig. 2 (a) Distributions of the values of the axial velocity component and (b) the z velocity component (perpendicular to the paper plane) for an eight-hole gas injector with 7 sLm of He flow and 10.97 sLm of Ar flow. $p = 1$ atm at the nozzle exit, and the actual velocities at the injection holes have been used. No slip conditions have been used for the wall boundaries.

distribution in the torch for flow injected with a straight flow injector. What is notable is that the flow shows a strong recirculation in the region where the Ar flow meets the He flow. Increasing the He flow rate moves the location of the recirculation upstream. Similar observations have been made for the flow with the four-hole swirl injector. Additionally, it was observed that the magnitude of the swirl velocity increases in the region where the He is injected. The flow pattern with the eight-hole swirl injector was similar to that with the four-hole swirl injector; however, the influence of an increase in the He flow rate was less pronounced, and there appeared to be a thinner boundary layer in the cylindrical part of the anode section. Figure 2 shows the distributions of the x velocity component (axial) and the z velocity component (perpendicular to the paper plane), indicating the increased swirl velocity and the slight recirculation.

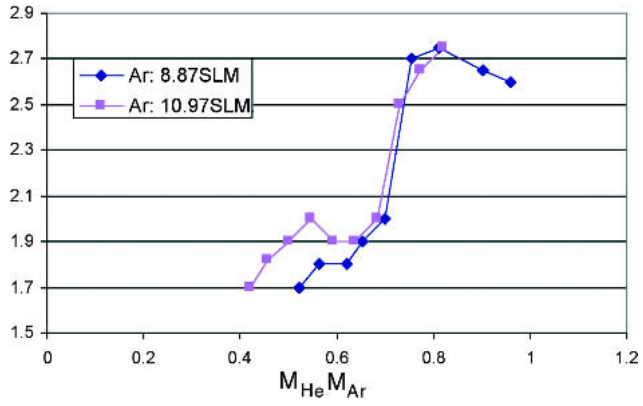

Fig. 3 Axial position of smoke deposition (distance from nozzle exit) as a function of the He-to-Ar mass flow rate ratio, showing a strong increase in distance at M_{He}:M_{Ar} of about 0.7.

4. Experimental Results

4.1 Cold Flow Experiments

Flow observation with the video camera shows a strong concentration of seed particles at certain locations and a rapid deposition of the particles at the wall at these locations. The locations of these depositions have therefore been investigated as the principal indication for the fluid dynamic patterns inside the torch. In the experiments with the four-hole straight gas injector, the deposition areas were located at the entrance of the cylindrical section of the anode nozzle, but were circumferentially nonuniform. The particles were deposited preferentially directly downstream at the same azimuthal location of the injection holes. The axial location of the deposits moved upstream with increasing He flow at constant Ar flow, and this upstream movement was less pronounced for higher Ar mass flow rates.

Use of the four-hole swirl injector results in a ring-shaped deposit region, however, the plane of the ring was tilted with respect to the torch axis (i.e., nonperpendicular to it). The distance of the deposit from the nozzle exit was a monotonically increasing function of the ratio of the He mass flow rate to argon mass flow rate. A particular large increase in this distance (i.e., a strong upstream movement of the deposition region) was seen when the standard volumetric flow rate ratio was around 0.7 (Fig. 3). Little change in the location occurred for He flow rates equal to or larger than the argon flow rates. With the eight-hole injector, the powder deposition was uniform up to the beginning of the straight part of the nozzle. For the lower He flow rates, there was also a deposit at the downstream end of the nozzle.

Figure 4 shows images of the glass nozzle with the deposits obtained with (a) a four-hole straight injector and (b) with a four-hole swirl injector. The velocity distributions obtained with the finite-element simulation for the corresponding flow conditions are placed above the images. The distance from the nozzle end to the downstream end of the deposit on the glass nozzle wall

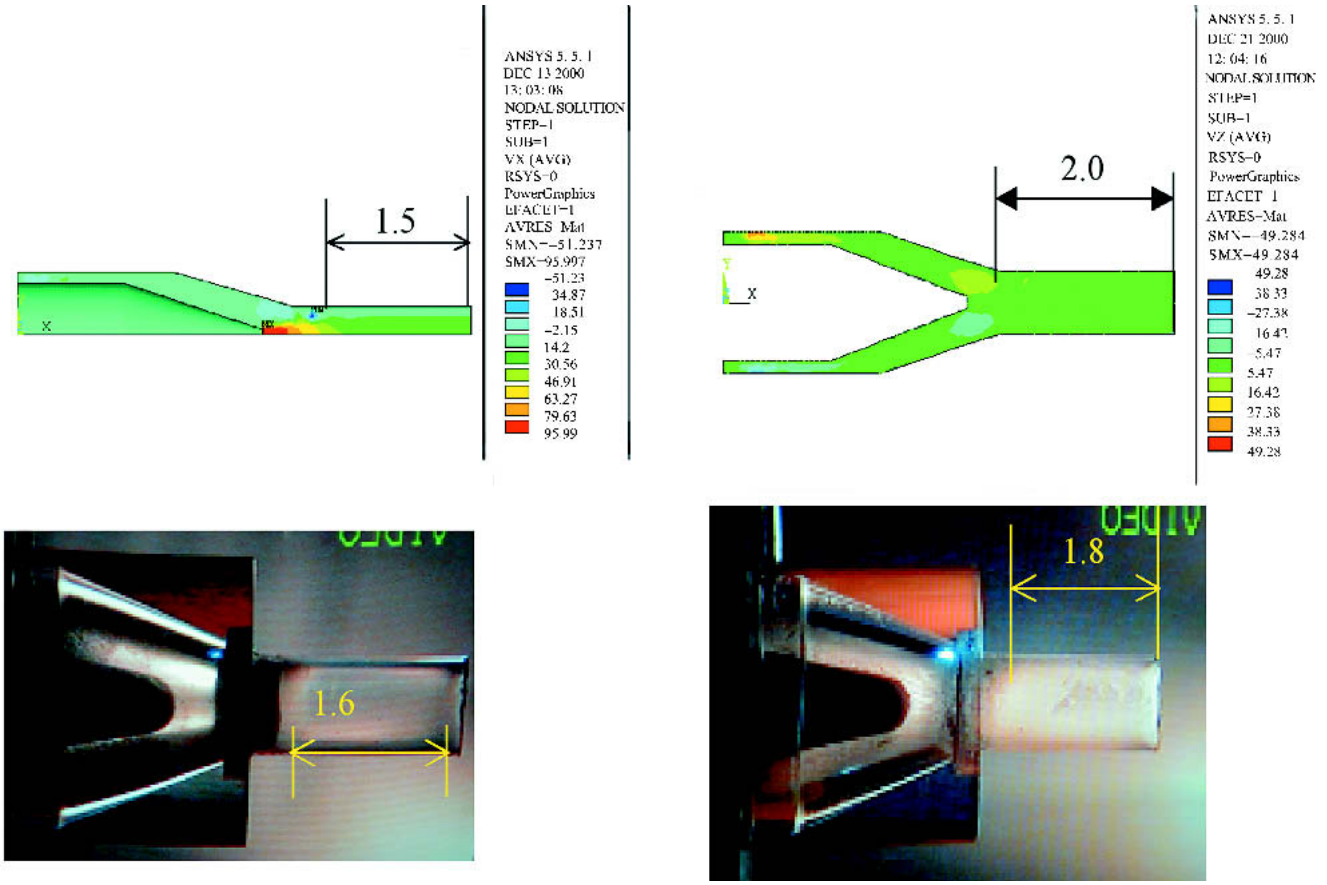

Fig. 4 Images of the glass anode nozzle with particle deposits and the corresponding velocity distributions above. (a) Straight flow injector with the axial velocity distribution. (b) Four-hole swirl injector with the distribution of the *z*-velocity component. The numbers on the distance marks indicate the distance from the nozzle exit in centimeters.

is typically between 15 and 20 mm, and it can be seen that this distance has almost the same value as the distance from the nozzle end to the recirculation eddies in the flow calculations. This behavior is consistent for all the different flow conditions. It is quite sensible that the recirculation eddies lead to mass transport from the central portions of the flow channel to the nozzle wall.

4.2 Plasma Torch Erosion

With a four-hole straight flow injector, the eroded surface area is localized at a single circumferential spot between two injection holes, and between axial distances from the nozzle exit of about 20 to 28 mm. The rotation of the injector ring by 45° results in a new erosion area, again between two injector holes. The erosion pattern with a four-hole swirl injector changes into a slanted ring covering three quarters of the circumference. The axial extent of the erosion area is from 26 to 15 mm from the nozzle exit. The erosion region moves upstream with a decreasing flow rate. The voltage traces during the torch operation did not show any effect of erosion (i.e., no distinct frequency has been observed in the power spectrum of the fluctuations) (Ref 11). The anode operated with the eight-hole swirl injector showed the least amount of erosion, distributed uniformly over the circumference and at axial locations similar to those observed with the four-hole swirl injector.

5. Discussion

The results show that there appears to be correlations among the recirculation region described in the cold-flow CFD simulation, the deposition of the powder on the wall in the cold-flow experiments, and the erosion pattern in the plasma torch. In Fig. 5, the results from the different studies are compared for the case of a four-hole swirl injector, with the powder deposition in the cold-flow experiments at the top, the distribution of the *z* component of the velocity below (i.e., the component out of or into the paper plane), and the sectioned plasma torch anode showing the erosion region at the bottom. The anode has been sectioned not in the midplane to show a larger part of the circumference and therefore to show more clearly the circumferential asymmetry of the erosion pattern. Powder deposition, recirculation, and erosion appeared at almost the same axial locations. It is apparent that the Ar flow from the base of the cathode encountered an obstacle at the location of the cathode tip where the He flow was emanating, simulating the arc-heated low-density gas. This obstacle caused a recirculation eddy in the Ar flow, as well as an increased vortex flow velocity in the case

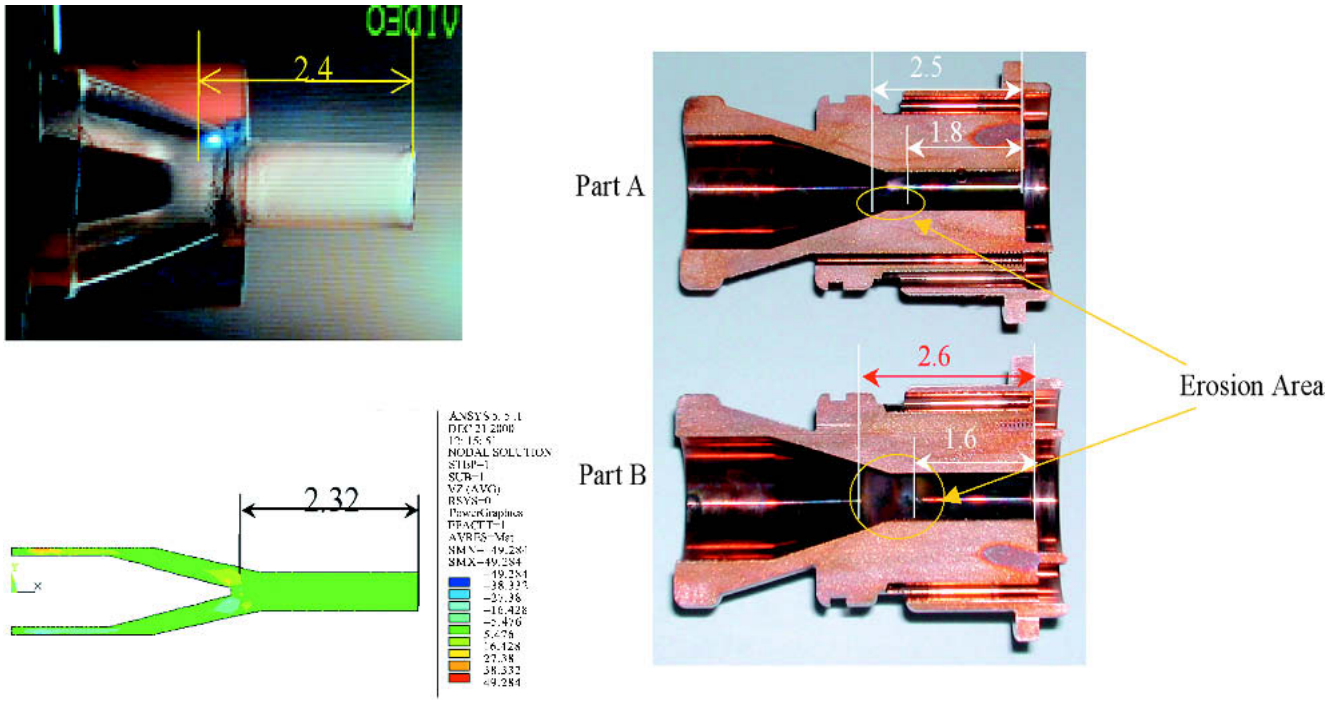

Fig. 5 Comparison of powder deposition region in the cold-flow experiment (top), the distribution of the *z* component of the velocity in the cold-flow CFD simulation, and images of a sectioned anode showing the erosion area. All results are for a four-hole swirl injector. The numbers in the space markers indicate the distance from the nozzle exit in centimeters.

of the swirl gas injection. Both effects led to an increase in the powder deposition on the wall. It is possible that the same effects led to a preferred anode attachment immediately downstream of their occurrence. Increasing He flow simulates increased arc current, with a stronger widening of the low-density plasma channel and an upstream movement of the recirculation region. To avoid the recirculation pattern, the channel between the arc at the cathode tip and the wall needs to be small and not converging (i.e., the cathode tip should be in the straight part of the anode nozzle). Obviously, for low gas flow rates the problem exists that the arc may attach upstream of the cathode tip, resulting in even stronger erosion.

Another interesting result is that the flow is, to a certain extent, stratified (i.e., the flows emanating from the different injection holes do not mix if there are only four holes). This effect was demonstrated by the fact that circumferential nonuniformities exist in both the powder deposition and the erosion patterns under these conditions. For the straight flow gas injector, the velocities exactly downstream of the injection holes are higher, leading to an arc attachment between the high-velocity streams. It is interesting to note that an existing erosion pattern at another location does not create a preferred attachment for the arc, but that the fluid dynamic condition dominates the location of the attachment. Also with the four-hole swirl injector, there is no uniformly rotating flow, but rather a circumferential velocity distribution that varies axially, as shown by the helical form of the particle-deposition region and the erosion region. It appears that an injector with eight or more holes must be used to achieve axial uniformity. Figure 6 summarizes schematically all of the observations for the different injectors, including the indication for the recirculation eddies, the deposition of the powder in the cold-flow experiments, and the areas of erosion. The distances from the nozzle exit are indicated for the different effects, and their values appear to indicate that these effects are related.

6. Summary and Conclusions

Low-temperature experiments have been performed with plasma spray torch geometry to study the fluid dynamics within the torch. These experiments have been supplemented by CFD simulations of the cold flow and by erosion measurements with actual plasma torches. The results indicate that:

- The low-temperature experiments and calculations provide some insight into the torch fluid dynamics.
- A recirculation region exists in which the gas flow meets the low-density plasma (simulated by the use of heated He in the low-temperature measurements).
- This recirculation affects the location of the arc anode attachment and consequently the erosion.
- There appears to be some stratification of the flow with a four-hole gas injector, resulting in circumferential variations of the axial velocity and, consequently, in preferred anode attachment regions with stronger erosion.

Minimizing the erosion effects would require (a) eliminating or at least minimizing the recirculation eddies by the proper design of the flow channel between the cathode and the anode, and (b) using gas injectors with eight or more holes to achieve adequate uniformity of the gas-velocity distributions.

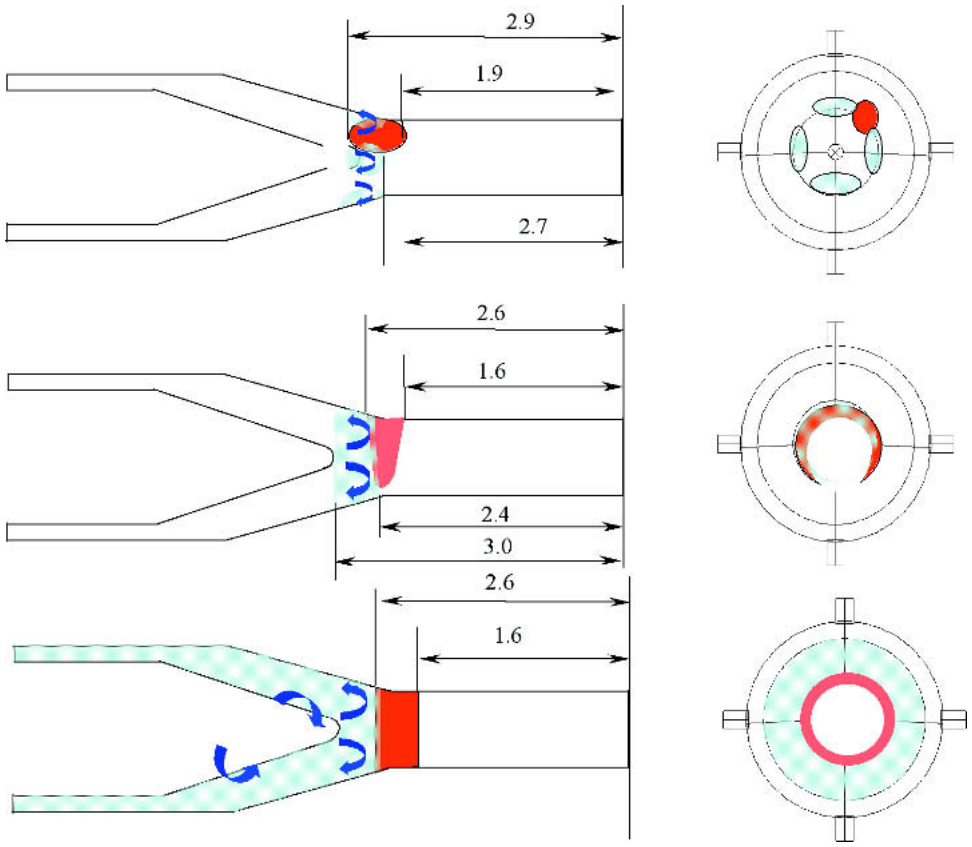

Fig. 6 Schematic indication of locations of the recirculation region (blue arrows), the powder deposition (light blue), and the erosion (red) in side view and cross section for the straight gas injector (top), the four-hole swirl gas injector (center), and the eight-hole swirl gas injector (bottom)

Acknowledgment

This research was supported in part by the National Science Foundation under grant number CTS-9903950 and CTS-0225962.

References

1. J. Zierhut, P. Halsbeck, K.D. Landes, G. Barbezat, M. Muller, and M. Schutz, Triplex: An Innovative Three-Cathode Plasma Torch, *Thermal Spray: Meeting the Challenges of the 21st Century,* C. Coddet, Ed., May 25-29, 1998 (Nice, France), ASM International, 1998, p 1375-1379
2. P. Fauchais, A. Vardelle, and B. Dussoubs, Quo Vadis Thermal Spray, *J. Therm. Spray Technol.,* Vol 10 (No. 1), 2001, p 44-66
3. B. Westhoff and J. Szekely, A Model of Fluid, Heat Flow an Electromagnetic Phenomena in a Nontransferred Arc Plasma Torch, *J. Appl. Phys.,* Vol 70, 1991, p 3455-3466
4. J.M. Bauchire, J.J. Gonzalez, and A. Gleizes, Modeling of a DC Plasma Torch in Laminar and Turbulent Flow, *Plasma Chem. Plasma Process.,* Vol 17 (No. 4), 1997, p 409-432
5. S. Paik, P. Huang, J. Heberlein, and E. Pfender, Determination of the Arc-Root Position in a DC Plasma Torch, *Plasma Chem. Plasma Process.,* Vol 13 (No. 3), 1993, p 370-397
6. H.P. Li and X. Chen, Three-Dimensional Modeling of a DC Non-Transferred are Plasma Torch, *J. Phys D: Appl. Phys.,* Vol 34, 2001, p L99-L102
7. H.P. Li, E. Pfender, and X. Chen, Applications of Steenbeck Minimum Principle for Three-Dimensional Modeling of DC Are Plasma Torches, *J. Phys. D: Appl. Phys.,* Vol 36, 2003, p 1084-1096
8. Mariaux, G.E. Legros, and A. Vardelle, "3-D Transient Modeling of a DC Plasma Spray Process," presented at Proc. Tenth CIMTEC International Ceramics Congress (Firenze, Italy), Vol F, P. Vicenzini, Ed., Tech. Sri, Florence, Italy. July 2002
9. X. Sun, "Investigations of Flow Fields Inside a DC Pasma Torch," M.S. thesis, University of Minnesota, 2002
10. R. Spores and E. Pfender, Flow Structure of a Turbulent Thermal Plasma Jet, *Surf. Coat. Technol.,* Vol 37, 1989, p 251
11. Z. Duan, L. Beall, M.P. Planche, J. Heberlein, E. Pfender, and M. Stachowicz, Arc Voltage Fluctuations as in Indication of Spray Torch Anode Condition, *Thermal Spray: A United Forum for Scientific and Technological Advances,* C.C. Berndt, Ed., Sept 15-18, 1997, ASM International, 1997, p 407-411